



OPERATING TEMPERATURES OF THE SOLAR CELLS USED IN THE CONCENTRATOR SYSTEM WITH RADIATING PLATES

Nevsan SENGİL*, Kurşad Melih GULEREN** and Uluc SENGİL***

*University of Turkish Aeronautical Association Aeronautical and Astronautical Science Faculty Aeronautical
Engineering Department 06790 Etimesgut, Ankara, Turkey, nsengil@thk.edu.tr

** Anadolu University, Faculty of Aeronautics and Astronautics,
26470 Tepebasi, Eskisehir, Turkey, kmguleren@anadolu.edu.tr

*** Koc University College of Sciences Department of Mathematics
34450 Sariyer, Istanbul, Turkey, usengil@koc.edu.tr

(Geliş Tarihi: 24.02.2015, Kabul Tarihi: 23.05.2016)

Abstract: A solar cell concentrator system is offered to satisfy the energy requirement of the satellites orbited around the Earth. The solar cells coupled to the system are exposed to sunlight concentrated 124 times with a Cassegrain type reflector system. To dissipate the waste heat to the space, the cells are bonded on a radiating plate. To calculate the temperature distribution on the surface of the radiating plate, a new FAS (Full Approximation Scheme) solver is developed. This new FAS solver is validated with the Newton method. Additionally, the FAS solver is shown to be 92 times more efficient computationally than the Newton method. Afterwards, radiating plate efficiencies are calculated. These efficiency figures change between 0.1 and 0.02 for different cell temperatures. Next, an energy balance equation is constructed in order to calculate the theoretical operating temperatures of the solar cells. Using energy balance equation and the FAS solver iteratively, solar cell operating temperatures are calculated successfully for different radiating plate thicknesses and solar cell conversion efficiencies. Solar cell operating temperatures are found between 500 K and 1000 K. The present study points out that concentrator systems require highly efficient solar cells operating in the very high temperatures. For instance, in order to operate the cell temperature at 750 K for a 3 mm radiating plate thickness, the cell conversion efficiency should be 70%. Ongoing projects which aim to develop solar cells capable of operating in high intensity-high temperature environments are believed to make it possible to embed solar cell concentrator systems on the next generation satellites.

Keywords: Solar cells, Antennas, Gallium Arsenide, Heat transfer, Satellite antennas, Renewable energy sources, Temperature control, Temperature measurement.

RADYASYON PANELLİ YOĞUNLAŞMA SİSTEMLERİNDE KULLANILAN GÜNEŞ HÜCRELERİNİN ÇALIŞMA SICAKLIKLARI

Özet: Dünya çevresinde yörüngede dönen uyduların enerji ihtiyacını karşılamak için bir yoğunlaşmalı güneş hücresi sistemi önerilmiştir. Cassegrain tipi bir yansıtıcı kullanılarak 124 defa yoğunlaştırılan güneş ışığı sistemde yer alan güneş hücrelerine yönlendirilmektedir. Artık ısı enerjisini uzaya aktarmak için güneş hücreleri bir radyasyon levhasına yapılandırılmaktadır. Radyasyon levhası yüzeyindeki sıcaklık dağılımını hesaplamak için yeni bir FAS çözücü geliştirilmiştir. Bu yeni FAS çözücü Newton yöntemi ile yapılan bir çözüm ile doğrulanmıştır. İlave olarak, FAS çözücünün Newton yöntemine nazaran 92 kez daha hızlı çalıştığı gösterilmiştir. Takiben, radyasyon levhasının ısı transferi verimliliği hesaplanmıştır. Verimliliğin hücre sıcaklığına bağlı olarak 0.1 ile 0.02 arasında değiştiği görülmüştür. Daha sonra, güneş hücrelerinin çalışma sıcaklığını hesaplamak için bir enerji denge denklemi oluşturulmuştur. Enerji denge denklemi ve FAS çözücüsünü birlikte ardışık çalıştırarak, güneş hücresi çalışma sıcaklıkları farklı radyasyon levha kalınlıkları ve güneş hücresi verimlilikleri için başarı ile hesaplanmıştır. Güneş hücresi çalışma sıcaklıklarının 500 K ile 1000 K arasında değiştiği görüldü. Bu çalışmada, yoğunlaşma sistemlerinde yüksek verimli ve yüksek sıcaklıklara dayanıklı güneş hücrelerinin kullanılması gerektiği belirlenmiştir. Örneğin 750 K çalışma sıcaklığı ve 3 mm kalınlığında bir radyasyon levhası için hücre verimliliğinin 70% olması gerekmektedir. Yüksek yoğunlukta ve yüksek sıcaklıkta çalışabilen güneş hücresi geliştirme projelerinden görülmektedir ki, gelecek nesil uydularda güneş hücresi yoğunlaştırma sistemlerinin kullanılması mümkün olacaktır.

Anahtar Kelimeler: Güneş hücreleri, Antenler, Galyum Arsenür, Isı transferi, Uydu antenleri, Yenilenebilir enerji kaynakları, Sıcaklık kontrolü, Sıcaklık ölçümü.

NOMENCLATURE

a	Position of the secondary focus [m]
A_c	Active solar cell area [m ²]
A_f	Radiating plate surface [m ²]
A_p	Primary concentrator area [m ²]
C	Concentration ratio
D_m	Diameter of the primary reflector [m]
e	Eccentricity
f	Half distance between focus and its image [m]
F	Focal distance of the primary reflector [m]
I_s	Solar power intensity [W/m ²]
k	Thermal conductivity [W m ⁻¹ K ⁻¹]
L	Length [m]
L_m	Phase center of the feed [m]
P_l	Incoming light power [W]
P_m	Maximum electric power [W]
s	Plate thickness [m]
T	Temperature [K]
T_{cell}	Cell temperature [K]
x, y, z	Spatial coordinates [m]

Greek Symbols

η	Conversion efficiency
θ_s	Angle between horizontal axis and edge ray on the secondary reflector [degree]
ϵ_0	Surface emissivity [W m ⁻¹ K ⁻¹]
σ	Stefan-Boltzmann constant [$\cong 5.67 \times 10^{-8}$ W m ⁻² K ⁻⁴]
θ	Dimensionless temperature
ϵ_c	Concentrator optical efficiency
Ω	Plate radiation efficiency

INTRODUCTION

Satellites and space vehicles can collect energy from the Sun. Currently, most of the satellites are equipped with solar cell panels, which run under direct sunlight without any concentration ($C=1x$). When the sunlight photons strike solar cells, some portions of the photon energy are converted over to electrical energy. The conversion efficiency of the solar cell (η) is defined as the ratio of the maximum electric power production (P_m) to the incoming light power (P_l),

$$\eta = \frac{P_m}{P_l}. \quad (1)$$

Solar cell efficiency is a function of the radiance intensity, the cell operating temperature and the incident spectrum (Fernandez *et al.*, 2014). The efficiencies of the solar cells vary considerably. While organic and dye type solar cell efficiencies are around $11.0 \pm 0.3\%$ and $11.9 \pm 0.4\%$ respectively, silicon solar cell efficiency can be as high as $25.6 \pm 0.5\%$ ($T=25^0$ C and $C=1x$). In case of multijunction devices (InGaP/GaAs/InGaAs), higher efficiencies ($37.9 \pm 1.2\%$) can be observed ($T=25^0$ C and $C=1x$) (Green *et al.*, 2015). Nevertheless,

these efficiencies are still quite low compared with the theoretical values of 70% (King *et al.*, 2012). One way to increase the solar cell efficiency is to build solar cell concentrator systems to concentrate the sunlight (Baig *et al.*, 2012). For example, the efficiencies of the multijunction devices (GaInP/GaAs; GaInAsP/GaInAs) can be much higher as $46.0 \pm 2.2\%$ under concentrated light ($T=25^0$ C and $C=508x$). Constructing solar cell concentrator systems for space application has some additional advantages. Foremost, these systems are more economical compared with the flat panel solar cell systems because concentrating mirrors or lenses are less expensive than the solar cells. Besides, because of the geometry, the concentrator system provides additional protection against space radiation and MMOD (micrometeoroids and orbital debris). These additional protections extend the lifespan of the solar cells (Bailey and Flood, 1998). On the other hand, the efficiency of the solar cells can be adversely affected by high operating temperatures, if excess heat produced by the concentrator system is not removed (Ho *et al.* 2011). Therefore, thermal management of the solar cells becomes rather important in designing concentrator systems. If not, high temperatures might affect both short and long term performance of the solar cells adversely (Royne *et al.*, 2005) or completely damage it (Nunez *et al.*, 2013). For the thermal management of the solar cells, either passive or active heat transfer systems can be employed to dissipate excess thermal energy to the space using radiating plates.

In this work, we suggest a solar cell concentrator system for satellites in Earth orbits and carry out a numerical analysis to predict the solar cell operating temperatures for different solar cell conversion efficiencies and radiating plate thicknesses. First, a Cassegrain-type concentrator system and a radiating plate are designed for a concentration ratio of 124x. Second, a nonlinear partial differential equation solver based on full approximation scheme (FAS) is developed to analyze radiation efficiency of the radiating plate. Then, an energy balance equation is constructed to estimate the steady solar cell operating temperature. Finally, utilizing the energy balance equation and FAS solver together, solar cell operating temperatures are specified for different radiating plate thicknesses and solar cell conversion efficiencies. These calculations give an approximation of the solar cell operating temperatures under 124x concentration with AM0 conditions.

CONCENTRATOR SYSTEM

Solar cell concentrator systems either use large area optical reflectors or refractor lenses or a combination of these to intercept sunlight (Chong *et al.*, 2013). Following, this sunlight is concentrated on a smaller area solar cell. Solar cell concentrators use tracking devices to follow the Sun. Depending on the light intensity, solar cell concentrators can be equipped with the cooling systems to extract excessive heat from the

system. They are classified according to their concentration ratio as low ($C < 40x$), medium ($40x < C < 300x$) and high ($300x < C < 2000x$) (Khamooshi *et al.*, 2014). Concentration ratio is defined as the ratio of primary concentrator area (A_p) to the active solar cell area (A_c), as indicated below Chemisana, 2011),

$$C = \frac{A_p}{A_c}. \quad (2)$$

The proposed solar cell concentrator consists of a cylindrical Cassegrain-type reflector and linearly positioned solar cells in the center of the radiating plates, as depicted in Figure 1.

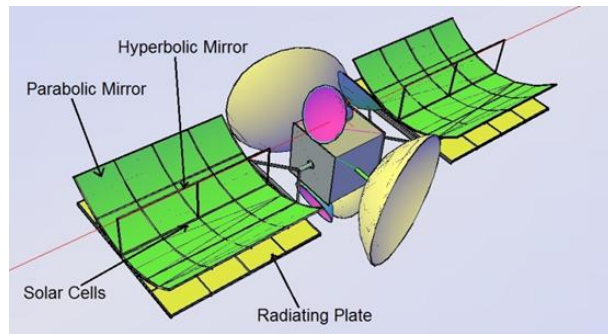


Figure 1. Satellite equipped with a solar cell concentrator system.

The size of the solar cell system is based on a parabolic cylinder reflector diameter ($D_m=10$ m) which is in same order of magnitude with the commercial communication satellites. This Cassegrain-type reflector system consists of two reflectors. The primary reflector is a parabolic cylinder, whereas the secondary reflector located at the focus of the cylinder is a hyperbolic line. Incoming sunlight is focused from primary parabolic reflector toward the secondary hyperbolic reflector. The secondary reflector further concentrates the sunlight onto the solar cells placed on the radiating plate. Secondary reflector position and size is chosen to avoid spillover and diffraction effects. Other parameters are calculated accordingly (Granet, 1998). These design parameters are presented in Table 1.

Table 1. Design parameters of the Cassegrain reflector.

D_m (m)	F/D_m	$2f/F$	e
10	0.3	5	1.0041
$L_s=a+f$ (m)	$L_m=F-2f$ (m)	θ_e ($^\circ$)	C
14.95	-12	0.1954	124

In Table 1, D_m , F , f , e , a , L_m , θ_e , and C are the diameter of the primary reflector, focal distance of the primary reflector, half distance between the focus and its image, eccentricity, position of the secondary focus, phase

center of the feed, angle between horizontal axis and edge ray on the secondary reflector, and concentration ratio respectively. Technical illustration of the solar cell concentrator system is depicted in Figure 2.

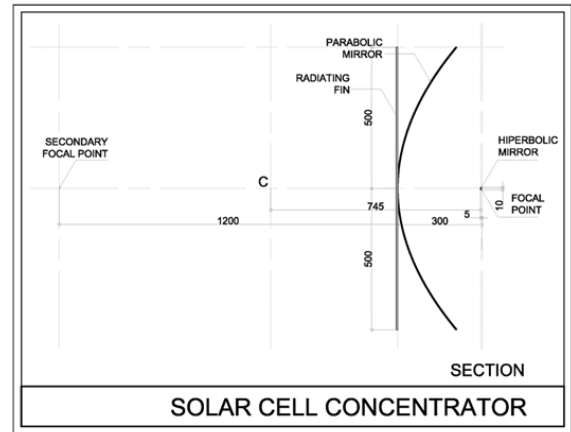


Figure 2. Technical drawing of the solar cell concentrator. The units are in centimeters.

THERMAL MANAGEMENT

Thermal management of the solar cell concentrating system is numerically analyzed to define the solar cell operating temperatures. The proposed concentrator system includes a radiating plate with constant thickness in order to cool the solar cells. The passive cooling with radiating plates is adopted because they are simple, economical and reliable. Power consumption of the active cooling techniques is generally higher than the power gains (Landis *et al.*, 2004). To analyze the heat transfer features of this system, first the temperature distribution on the radiating plate should be set.

Solar cells are placed on a metal-radiating plate located behind the primary parabolic mirror. Aluminum (Al) is adopted as a metal because of its low thermal resistance, mass density and cost. Thermal energy is delivered to the radiating plate through conduction. It is assumed that the contact between solar cells and the radiating plate is excellent (no thermal resistance) and the temperature distribution throughout the solar cells is homogeneous. Thermal conductivity (k) and surface emissivity (ϵ_0) are not temperature dependent. The schematic representation of the solar cells and upper half of the radiating plate is presented in Figure 3.

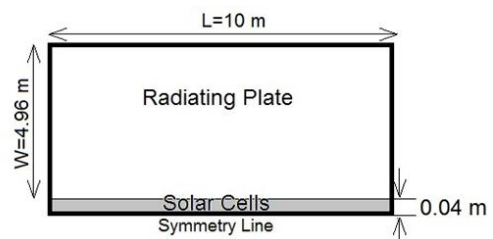


Figure 3. Geometric representation of the radiating plate.

In order to calculate the temperature distribution, the heat transfer equation corresponding to the current problem should be built. This is a steady nonlinear boundary value problem which incorporates radiation and conduction modes of the heat transfer as shown below,

$$\frac{\partial^2 T}{\partial x^2} + \frac{\partial^2 T}{\partial y^2} + \frac{\partial^2 T}{\partial z^2} = \frac{\sigma \varepsilon_0}{k s} (T^4 - T_e^4). \quad (3)$$

In Eq. (3), T , T_e , x , y , z , σ , ε_0 , k and s are temperature, vacuum temperature, spatial coordinates, Stefan-Boltzmann constant, surface radiation emissivity, thermal conductivity, and thickness of the plate, respectively. If the thickness is rather low ($s \ll W, s \ll L$) in comparison to the width ($W = 4.96 \text{ m}$) and length ($L = 10 \text{ m}$) of the plate, partial differential equation can be considered two dimensional as shown below (Howell *et al.*, 2002),

$$\frac{\partial^2 T}{\partial x^2} + \frac{\partial^2 T}{\partial y^2} = \frac{\sigma \varepsilon_0}{k s} (T^4 - T_e^4), \quad (4)$$

with boundary conditions,

$$\begin{aligned} \frac{\partial T}{\partial x}(0, y) = 0, \quad \frac{\partial T}{\partial x}(L, y) = 0, \\ \frac{\partial T}{\partial y}(x, W) = 0, \quad T(x, 0) = T_{cell}. \end{aligned} \quad (5)$$

These boundary conditions can be represented as in Figure 4.

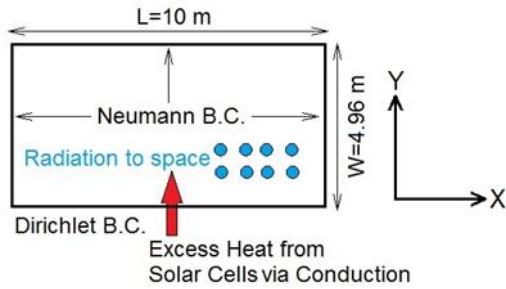


Figure 4. Boundary conditions for the upper part of radiating plate.

Neumann boundary conditions represent an adiabatic (no heat transfer) boundary condition on the left, right, and upper boundaries, whereas all the conduction heat transfer is realized through the lower boundary with Dirichlet boundary condition. This excess heat is transferred to the space environment from only back side of the plate through radiation.

In this specific case, we presumed that the vacuum temperature (T_e) is equal to 0 K. Therefore, the

governing equation of the heat transfer problem becomes,

$$\frac{\partial^2 T}{\partial x^2} + \frac{\partial^2 T}{\partial y^2} = \frac{\sigma \varepsilon_0}{k s} T^4. \quad (6)$$

Eq. (6) can be further converted to a dimensionless form. New dimensionless variables are $\theta = T/T_0$, $Y = y/W$, $X = x/L$. Dimensional variables are presented as $T = T_0 \cdot \theta$ and $y = W \times Y$, $x = L \times X$. Utilizing these new variables, the dimensionless heat transfer problem becomes (Naumann, 2004),

$$\frac{\partial^2 (T_0 \times \theta)}{\partial (L \times X)^2} + \frac{\partial^2 (T_0 \times \theta)}{\partial (W \times Y)^2} = \frac{\sigma \varepsilon_0}{k s} (T_0 \times \theta)^4 \quad (7)$$

with boundary conditions,

$$\begin{aligned} \frac{\partial \theta}{\partial X}(0, Y) = 0, \quad \frac{\partial \theta}{\partial X}(L, Y) = 0, \\ \frac{\partial \theta}{\partial Y}(X, W) = 0, \quad \theta(X, 0) = T_{cell} / T_0 = \theta_{cell}. \end{aligned} \quad (8)$$

We can further simplify Eq. (7) as,

$$\frac{1}{L^2} \frac{\partial^2 \theta}{\partial X^2} + \frac{1}{W^2} \frac{\partial^2 \theta}{\partial Y^2} = T_0^3 \frac{\sigma \varepsilon_0}{k s} \theta^4. \quad (9)$$

If the values of the $T_0 (= 300 \text{ K})$, σ , $\varepsilon_0 (= 0.8)$, $k (= 237 \text{ W m}^{-1} \text{ K}^{-1})$, $s (= 0.003 \text{ m})$ are placed in the differential equation, we derive,

$$\frac{1}{L^2} \frac{\partial^2 \theta}{\partial X^2} + \frac{1}{W^2} \frac{\partial^2 \theta}{\partial Y^2} = 1.723 \theta^4. \quad (10)$$

As seen from the Figure 4 and Eq. (8), symmetry exists in the x-direction, because of the same Neumann boundary conditions. If this symmetry is taken into account as a special case, the length of the radiating plate can be chosen arbitrarily as $L = W$. Using this new condition, Eq. (9) changes to,

$$\frac{\partial^2 \theta}{\partial X^2} + \frac{\partial^2 \theta}{\partial Y^2} = 1.723 W^2 \theta^4 = 42.38 \theta^4. \quad (11)$$

To solve this nonlinear differential equation, Newton method can be used (Kelley, 1987). In the first place, a nonlinear algebraic equation system is constructed ($A(\mathbf{u}) = \mathbf{f}$) using finite difference scheme. Next, convergence to the solution is realized through the,

$$v_{i,j} \leftarrow v_{i,j} - \frac{f(x_i, y_j)}{f'(x_i, y_j)}, \quad (12)$$

iterations on each grid point. Iterations are ended when the residual ($\mathbf{r} = \mathbf{f} - A(\mathbf{v})$) become smaller than a predetermined value. Newton method is computationally expensive. We developed a new solver based on the FAS (Full Approximation Scheme) method (Briggs *et al.*, 2000) in order to solve Eq. (11) more efficiently.

FAS Method

FAS is a variant of the multigrid method (Trottenberg *et al.*, 2011). The main idea of FAS method is to start with a guessed solution (v_h) on the fine-grid (h) and try to smooth the error with a few iterations of Newton method. Gradually to eliminate the high frequency errors, then, restrict the approximation ($v_{2h} = I_h^{2h} v_h$) and residue ($r_{2h} = I_h^{2h} r_h$) to the coarse-grid ($2h$). This time, coarse-grid problem is solved (u_{2h}) and error values ($e_{2h} = u_{2h} - v_{2h}$) are interpolated back to the fine grid and approximation values are further corrected ($v_h = v_h + I_{2h}^h e_{2h}$). Repeating these operations many times in cycles, the solution converges. Once the average residue is smaller than the predetermined value we stop the calculations. We used V-type cycles in our FAS solver. The schematic representation of the FAS method and V-type cycle are presented in Figure 5 (Trottenberg *et al.*, 2011).

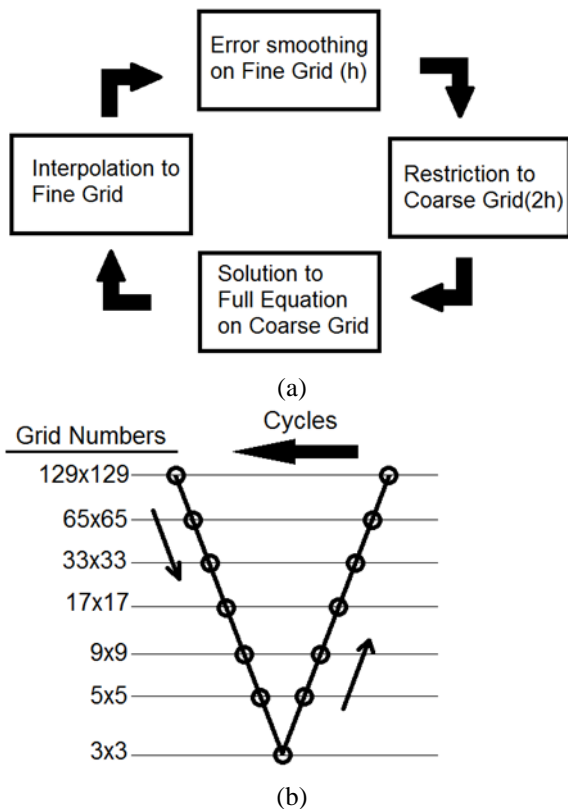
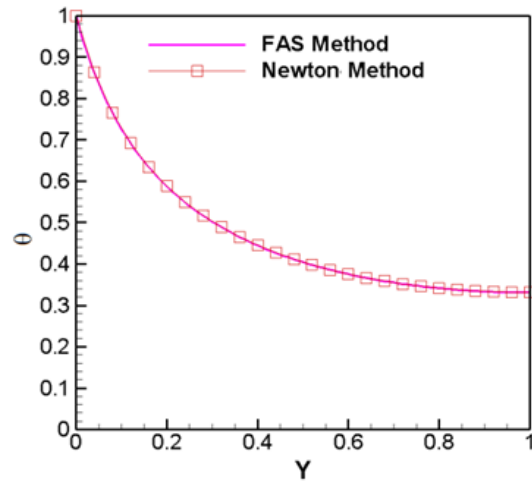


Figure 5. (a) Four main steps of the FAS method (b) V-type restriction-interpolation cycle.

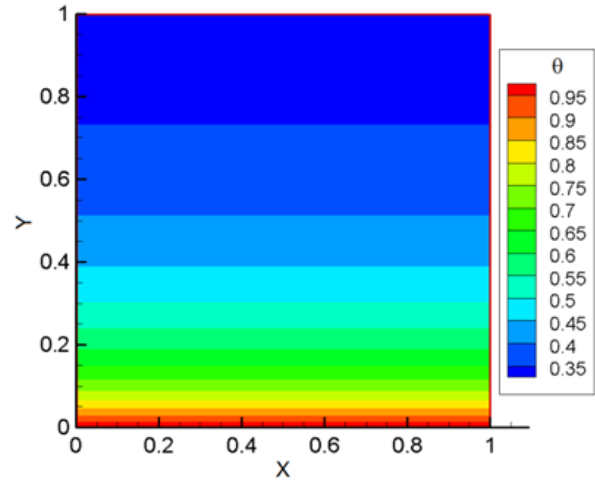
Newly developed FAS solver can be applied to two-dimensional nonlinear heat transfer problems containing

both Dirichlet and Neumann boundary conditions. To show the accuracy and the efficiency of the FAS solver, the same differential equation is also solved by the Newton method.

Temperature distributions obtained by these two methods are shown in Figure 6, and an excellent agreement is observed.



(a)



(b)

Figure 6. (a) Validation of the FAS with Newton method for $s=0.003$ m. (b) FAS solution of the two-dimensional temperature distribution on the radiating plate for $s=0.003$ m.

Computation times are 91 s for Newton method and 0.99 s for the FAS method. In the FAS method, 12 cycles are used for a 6.8×10^{-5} average residual value. On the other hand, in Newton method 59.000 iterations are used to achieve an average residual value 6.3×10^{-5} . A total of 16.641 (129x129) grid points are used in the computational domains of both FAS and Newton methods. Computations are executed on a PC (Intel i3 CPU with 4 GB memory). A summary of the

computation times and residuals of these two methods are displayed in Table 2.

Table 2. Computational efficiency of the FAS solver.

Method	Computation Time (s)	Cycle/Iteration	Average Residual
FAS	0.99	12	6.8×10^{-5}
Newton	91	59000	6.3×10^{-5}

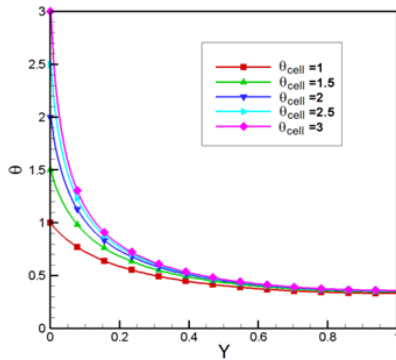
Following the solution of the heat transfer equation, plate radiating efficiency (Ω) is calculated.

The plate radiating efficiency is the ratio of the actual radiated energy to the radiated energy with base temperature (θ_{cell}) (Howell *et al.*, 2002).

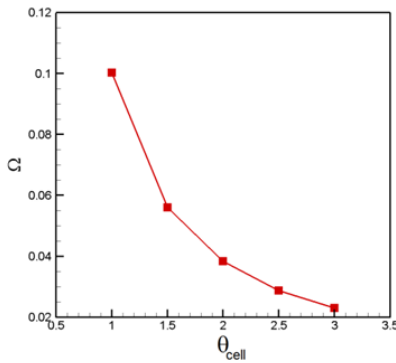
Because of the discrete values of the temperature ($\theta(i, j)$), radiated energy is calculated numerically,

$$\Omega = \frac{\int_0^1 \int_0^1 \theta^4(X, Y) dX dY}{\theta_{cell}^4 \times 1 \times 1} = \frac{1}{N^2} \sum_{i=1}^N \sum_{j=1}^N \theta^4(i, j). \quad (13)$$

Using Eq. (13), temperature distributions and the radiating plate efficiencies for the different cell temperatures are computed and presented in the plots as in Figure 7.



(a)



(b)

Figure 7. (a) Temperature distributions and (b) Radiating plate efficiencies for different cell temperatures.

Solar Cell Operating Temperature

To estimate the solar cell operating temperature, power input to solar concentrator systems and power output to space are calculated, and these equations are iterated to determine the solar cell operating temperature.

The thermal power input to the concentrator system is calculated as,

$$P_i = A_c I_s \varepsilon_c (1 - \eta). \quad (14)$$

In Eq. (14), A_c ($= 4.96 \times 10 m^2$), I_s ($= 1345 W m^{-2}$), ε_c , and η are primary surface area of the concentrator system, solar power intensity, concentrator optical efficiency and solar cell conversion efficiency, respectively (Kaushika and Reeta, 2011).

Optical efficiency is the power ratio of the intercepted solar light and reflected solar light.

Optical efficiencies are generally changes between 0.8 and 0.9 (Pereira *et al.*, 2014), but we keep this value equal to 1 ($\varepsilon_c = 1$) not to change the concentration ratio ($C = 124x$).

Second, power radiation transfer to the vacuum is calculated as,

$$P_o = A_f \sigma \varepsilon \Omega T_{cell}^4. \quad (15)$$

In Eq. (15), A_f ($= 5 \times 10 m^2$) and T_{cell} are radiating plate surface area and solar cell operating temperature.

Once power balance is obtained ($P_i = P_o$), the operating temperature of the solar cells can be computed from,

$$T_{cell} = \sqrt[4]{\frac{A_c I_s \varepsilon_c (1 - \eta)}{A_f \sigma \varepsilon \Omega}}. \quad (16)$$

In Eq. (16), plate radiation efficiency (Ω) is not a constant value, but depends on the cell temperature ($\Omega = \Omega(T_{cell})$).

If we place the constant values in the equation, we find,

$$T_{cell}^4 \Omega(T_{cell}) = 2.94 \times 10^{10} (1 - \eta) \quad (17)$$

Therefore, an iteration process is required to solve this problem.

The solar cell operating temperature and plate radiating efficiencies for different conversion efficiencies are plotted in Figure 8.

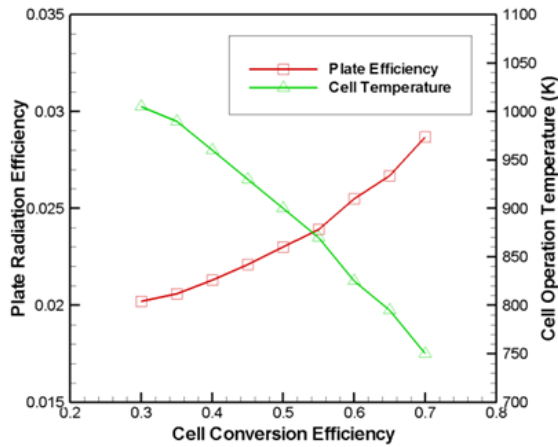


Figure 8. Plate radiation efficiencies and cell operating temperatures for different cell conversion efficiencies ($s=0.003$ m).

Cell operating temperatures are found to be very high between 750 K and 1000 K. These figures show that there is a need for higher efficiency solar cells operating in these high temperatures. Many programs are in progress to develop solar cells operating at high intensity, high temperature (HIHT) environments, without degradation, including GaInP, GaN, SiC and GaP cells (Landis, 2008). In addition to the solar cell concentrators, inner planet missions in the solar system such as Mercury missions require the use of such solar cells. High-temperature contacts for GaAs/Ge cells were developed to withstand 550°C ($\cong 823\text{ K}$) to counter laser illumination (Reed *et al.*, 1991; Iles, 2001). A recent study held at Yale University aims to develop dual-junction solar cells that can work efficiently at temperatures above 400°C ($\cong 673\text{ K}$) (Internet, 2014). In another study, solar cells exposed temperatures between 470 K and 500 K with 11 solar constants 470 h and 240 h respectively (Zimmermann *et al.*, 2013). Still, these new solar cells are not ready to withstand the operating temperature of our proposed concentrator system. In the next section, the thickness of the radiating plate is increased to reduce the thermal load of the solar cells.

Varying the Radiating Plate Thickness

In this part of the study, the radiation efficiency of the radiating plate is calculated for the different thicknesses of the plate. We increased the radiating plate thickness to decrease the cell temperature further down, and record the cell operating temperatures.

In Figure 9, operating temperatures of the solar cells are calculated for different solar cell conversion efficiencies ($0.3 \leq \eta \leq 0.7$) and plate thicknesses ($0.003\text{ m} \leq s \leq 0.03\text{ m}$). Although solar cell operating temperature is reduced between 500 K and 700 K, these values are nevertheless eminent.

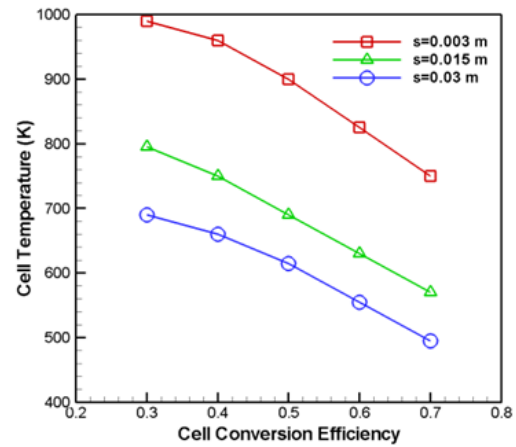


Figure 9. Effects of the radiating plate thickness and the cell conversion efficiencies for the cell operating temperatures.

The remaining thickness values (s) are not included since they are either too thin to break or too heavy for space applications (Min *et al.*, 2012). This figure clearly indicates that we should either use higher efficiency solar cells or increase the thickness of the radiating plate to decrease the operating temperature of the solar cells. In space applications, the weightiness of the radiating plate is real important in addition to its production cost because the launching cost of the satellites is directly linked to their weights. The width and length of the radiating plate are restricted by the concentrator system dimensions. As a result, changing the thickness and material of the radiating plate is the only option to increase the conduction rate to improve the radiating plate efficiency. We prefer Aluminum because the ratio of its thermal conductivity and density is approximately 87.8. This value proves more effective compared to copper ($\cong 43.5$) and steel ($\cong 5.4$).

CONCLUSIONS

Solar cell concentrator systems have some distinct advantages compared to the conventional arrays such as higher conversion efficiency, low cost and extra protection against space radiation and MMOD. Nevertheless, under HIHT conditions, operating temperatures of the solar cells can be quite high. High operating temperatures cause short or long term adverse effects on the solar cells. In this work, we suggest a solar cell concentrator system with 124x concentration ratio and passive radiating plate for cooling purposes. A new FAS solver is developed to calculate the operating temperatures of the solar cells under concentrated solar light. This new FAS solver is validated with the more familiar Newton method. Under AM0 conditions, our calculations show solar cells should operate in temperatures between 500 K and 1000 K depends on the solar cell conversion efficiency ($0.3 \leq \eta \leq 0.7$) and radiating plate thicknesses ($0.003\text{ m} \leq s \leq 0.03\text{ m}$). Ongoing projects justify that a high interest exists for

highly efficient solar cells function at high temperatures. In the very near future, we definitely expect that solar cell companies will produce highly efficient solar cells that operate at very high temperatures. These high temperature-high efficiency solar cells take out the most significant obstacle to make the solar cell concentrator systems with high concentration ratios.

ACKNOWLEDGMENT

The author would like to thank B. Yesim Sengil for the CAD drawings and artwork.

REFERENCES

Baig H., Heasman K. C., Mallick T. K., 2012, Non-uniform illumination in concentrating solar cells, *Renew. Sust. Energ. Rev.*, 16, 5890-5909.

Bailey S. G., Flood D. J., 1998, Space photovoltaics, *Prog. Photovoltaics*, 6, 1-14.

Briggs W. L., Henson, W. E., McCormick, S. F., 2000, *A Multigrid Tutorial*, SIAM, Philadelphia.

Chemisana D., 2011, Building Integrated Concentrating Photovoltaics: A review, *Renew. Sust. Energ. Rev.*, 15, 603-611.

Chong K-K., Lau S-L., Yew T-K., Tam, P. C-L., 2013, Design and development in optics of concentrator photovoltaic system, *Renew. Sust. Energ. Rev.*, 19, 598-612.

Fernandez E. F., Rodrigo P., Almonacid F., Perez-Higueras P., 2014, A method for estimating cell temperature at the maximum power point of a HCPV module under actual operating conditions, *Sol. Energ. Mat. Sol. C.*, 124, 159-165.

Granet C., 1988, Designing axially symmetric Cassegrain or Gregorian dual-reflector antennas from combinations of prescribed geometric parameters, *IEEE Antennas Propag.*, 40 (2), 76-82.

Green M. A., Emery K., Hishikawa Y., Warta W., Dunlop, E. D., 2015, Solar cell efficiency tables (Version 45), *Prog. Photovoltaics*, 23, 1-9.

Ho T., Samuel S. M., Greif R., 2011, The impact of cooling on cell temperature and the practical solar concentration limits for photovoltaics, *Int. J. Energ. Res.*, 35, 1250-1257.

Howell J. R., Siegel R., Menguc, M. P., 2002, *Thermal Radiation Heat Transfer*, Taylor & Francis, New York.

Iles P.A., 2001, Evolution of space solar cells, *Sol. Energ. Mat. Sol. C.*, 2001, 68, 1-13.

Internet, 2014, Arpa-e, *Dual-Junction Solar Cells for High-Efficiency at Elevated Temperature*, <http://www.arpa-e.energy.gov>

Kaushika N. D., Reeta, 2011, Simulation Model for High Efficiency of Solar Cells, *Energy Science and Technology*, 2 (1), 57-61.

Kelley C. T., 1987, *Solving Nonlinear Equations with Newton's Method (Fundamentals of Algorithms)*, SIAM, Philadelphia.

Khamooshi M., Salati H., Egelioglu F., Faghiri A.H., Tarabishi, J., Babadi S., 2014, A Review of Solar Photovoltaic Concentrators, *Int. J. Photoenergy*, 958521.

King R. R., Bhusari D., Larrabee D., et al., 2012, Solar cell generations over 40% efficiency, *Prog. Photovoltaics*, 20, 801-815.

Landis G. A., Jenkins, P., Scheiman, D., Rafaele, R., 2004, Extended Temperature Solar Cell Technology Development, *Proc. of AIAA 2nd International Energy Conversion Engineering Conference*, Providence, RI.

Landis G. A., 2008, Solar Power for Near-Sun; High-Temperature Missions, *Proc. of IEEE Photovoltaic Specialist Conference*, San Diego, CA, 1-5, 4922857.

Min C., Nuo-Fu C., Jin-Xiang D., 2012, Thermal modeling and optimized design of metal plate cooling system for single concentrator solar cells, *Chinese Phys. B*, 21 (3), 034216.

Naumann R. J., 2004, Optimizing the Design of Space Radiators, *Int. J. Thermophys.*, 25, 1929-1941.

Nunez N., Gonzales J. R., Vazquez, M., Algora, C., Espinet, P., 2013, Evaluation of the reliability of high concentrator GaAs solar cells by means of temperature accelerated aging tests, *Prog. Photovoltaics*, 21, 1104-1113.

Pereira A., Dargent L., Lorin G, et al., 2014, Electro-optical study of a x1024 concentrator photovoltaic system, *Prog. Photovoltaics*, 22, 383-393.

Reed B., Iles P., Krogen J., 1991, High temperature contact for GaAs solar cells, *Proc. of IEEE Photovoltaic Specialists Conference*, Las Vegas, NV, 450-454.

Royne A., Dey C. J., Mills D. R., 2005, Cooling of photovoltaic cells under concentrated illumination: a critical review, *Sol. Energ. Mat. Sol. C.*, 86, 451-483.

Trottenberg U., Oosterlee C. W., Schuller A., 2000, *Multigrid*, Academic Press, London.

Zimmermann C. G., Nömayr C., Kolb M., Rucki A., 2013, A mechanism of solar cell degradation in high intensity, high temperature space missions, *Prog. Photovoltaic*, 21, 420-35.



Nevsan ŞENGİL was born in Istanbul, in 1959. He received the B.S. degree in control systems from the Naval Academy, Istanbul, in 1980, the M.S. degree in engineering science from the Naval Postgraduate School, Monterey, CA, in 1986, and the Ph.D. degree in astronautical engineering from Istanbul Technical University, Istanbul, in 2008. He is currently a Faculty Member with the Department of Astronautical Engineering, University of Turkish Aeronautical Association, Ankara. His current research interests include particle simulations of gas, plasma flows, and electromagnetic launchers. Dr. Sengil is a member of the AIAA, IEEE and ACM.



Kürşad Melih GÜLEREN received B.Sc. degree in Aeronautical Engineering, Middle East Technical University in 1999 and then completed Masters education in Mechanical Engineering, Cumhuriyet University in 2003. Masters Thesis was about the numerical analysis of turbulent flow in a centrifugal pump. He started his Ph.D. in Mechanical Engineering, University of Manchester and completed his Ph.D. education in 2007. The Ph.D. thesis was about the Large Eddy Simulation of the flows subjected to curvature and rotation. He has been working for the Anadolu University in the Faculty of Aeronautics and Astronautics since 2016. His main research fields are aerodynamics, turbomachinery, computational fluid dynamics, flow control and aircraft design.



Uluç ŞENGİL was born in Ankara, Turkey, in 1992. He is currently pursuing the Science degree in mathematics and physics with Koc University, Istanbul. His current research interests include Monte Carlo methods and nonlinear differential equations. Mr. Sengil received a Full Scholarship from Koc University, and also received an additional scholarship from the Scientific and Technological Research Council of Turkey.